

## CRYSTAL STRUCTURE OF MAGNESIUM-VERMICULITE

A. McL. MATHIESON AND G. F. WALKER, *Division of Industrial Chemistry, Commonwealth Scientific and Industrial Research Organization, Melbourne, Australia.*

### ABSTRACT

A single-crystal *x*-ray analysis of Mg-vermiculite has located the interlamellar water molecules and exchangeable cations in definite positions with respect to the adjacent silicate layer surfaces. The exchangeable cation sites lie in a plane midway between silicate layers. The water network consists of two sheets, each arranged in a distorted hexagonal pattern. The water molecule sites are determined by the surface configuration of the silicate layers, each water being linked by a hydrogen bond to a single oxygen in the silicate layer surface. Weak hydrogen-bonding operates within individual water sheets. The water sheets are held together by the exchangeable cations, around which the water molecules tend to form hydration shells. The importance of the hydration behaviour of the cations rather than direct electrostatic interaction between cations and silicate layer surfaces in locating the cations is emphasized.

A regular distortion of the surface oxygen network of the silicate layers from the ideal hexagonal form is revealed by the diffraction data.

Vermiculite must be regarded as a true clay mineral since it is formed in the clay fractions of certain soils (Walker, 1950*a*). The characteristic properties of this mineral, such as high cation exchange capacity (Walker, 1947, 1949; Barshad, 1948), the ability to form complexes with organic substances (Walker, 1950*b*; Barshad, 1952) and a variable interlamellar distance depending on the exchangeable cation present and the humidity of the sample (Barshad, 1949; Milne and Walker, 1950; Walker, 1951), bear a striking resemblance to those of montmorillonite. This similarity, moreover, extends to their structures which, in so far as they are known, consist of complex silicate layers interleaved with layers of water molecules carrying exchangeable cations.

The detailed structure analysis of montmorillonite has been prevented mainly by the small grain size of the particles, and the configuration of the interlamellar water molecules and exchangeable cations in this mineral is not well understood. Mg-vermiculite, on the other hand, is available in large flakes (derived by the hydrothermal alteration of biotite and phlogopite) which are suitable for investigation by single-crystal *x*-ray methods. Vermiculite therefore seems to offer a promising line of approach to the general problem of the configuration of water molecules and exchangeable cations in the vicinity of layer silicate surfaces, and the present investigation was undertaken primarily with this aim in view. From the analysis, certain new features of the internal structure of the silicate layers and of the relationships between adjacent

silicate layers have appeared which are not in accord with previous views.

Earlier workers on the crystal structure of vermiculite (Gruner, 1934, 1939; Hendricks and Jefferson, 1938*a*) were in general agreement regarding the structure of the silicate layers and their relative disposition when viewed along the *b* axis, but neither obtained experimental evidence of the structure of the interlamellar water layers. Hendricks and Jefferson (1938*b*) proposed a hypothetical structure for the interlamellar water which was based partly on Bernal and Fowler's (1933) concept of the tetrahedral charge distribution of a water molecule in liquid water. Neither Gruner nor Hendricks and Jefferson were aware, at the time of their work, of the high cation exchange capacity of vermiculite, and more complete information on the dehydration characteristics of the mineral has since become available.

#### EXPERIMENTAL

The vermiculite used came from Kenya and was obtained through the courtesy of Mr. G. E. Howling of the Imperial Institute, London. The sample has a cation exchange capacity of 130 milliequivalents per 100 grams, all the exchange positions being occupied by  $Mg^{2+}$  ions. The chemical analysis (Table 1) shows no alkalis, indicating that no interleaved layers of mica are present. Small sections, free from cracks, were cut from cleavage flakes and gently pressed flat to minimize any distortion arising from the cutting operation. The approximate dimensions of the crystals used in obtaining the diffraction data were  $0.5 \times 0.2 \times 0.2$  mm.

Rotation films indicated that, for the three 9.18 Å axes disposed at

TABLE 1. CHEMICAL ANALYSIS AND FORMULA OF KENYA VERMICULITE  
(air dry)

	Wt. %
SiO <sub>2</sub>	34.04
Al <sub>2</sub> O <sub>3</sub>	15.37
Fe <sub>2</sub> O <sub>3</sub>	8.01
MgO	22.58
CaO	0.00
Na <sub>2</sub> O	0.00
K <sub>2</sub> O	0.00
H <sub>2</sub> O	19.93
	99.93
	$Mg^{2+}_{0.32}$
	↑
	(Mg <sub>2.36</sub> Fe <sup>+3</sup> <sub>0.48</sub> Al <sub>0.16</sub> ) (Al <sub>1.28</sub> Si <sub>2.72</sub> ) O <sub>10</sub> (OH) <sub>2</sub> · 4.32 H <sub>2</sub> O
Or	$[C_3D_4O_{10}(OH)_2]^{-0.64} [4.32H_2O \cdot 0.32 Mg^{2+}]^{+0.64}$

120° with respect to each other in the cleavage plane, the sharp  $3n$ -layer line spectra coincide in position and intensity, but that marked differences occur in the intensity distribution of the  $(3n \pm 1)$ -layer spectra. Oscillation films disclosed only one axis with equivalence of both sharp and diffuse  $+n$ - and  $-n$ -layer spectra. The crystal system is therefore monoclinic. Moving films of the zero, first, second and third layers about the  $b$ -axis were recorded on an equi-inclination Weissenberg goniometer (Mathieson, 1951). The cell constants obtained are in good agreement with those of Gruner (1934), but differ from those of Hendricks and Jefferson (1938a) in the selection of the  $\beta$ -angle.

	Gruner	Hendricks and Jefferson	Mathieson and Walker
$a$	5.3	5.33	5.33 Å
$b$	9.2	9.18	9.18 Å
$c$	28.57-28.77	28.85	28.90 Å
$\beta$	97°09'	93°15'	97°
Space Group	$Cc$ or $C2/c$	$Cn$ or $C2/n^*$	$Cc$

\* Reported as  $Cc$  or  $C2/c$ .

Comparison of the  $h0l$  and  $h3l$  moving-film photographs shows that, for  $\beta=97^\circ$ , the unit cell corresponding to the sharp  $k=3n$  spectra is centered on the  $C$  face and contains one silicate layer ( $c=14.45$  Å). Inclusion of the diffuse  $k \pm 3n$  spectra requires a doubling of the  $c$  axis

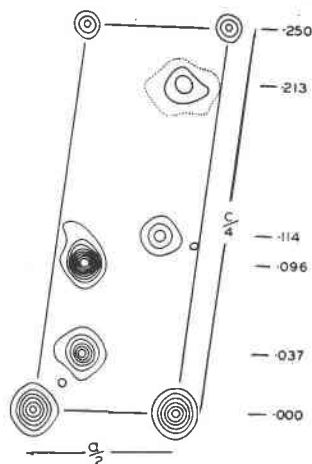


FIG. 1. (a) Electron-density distribution on (010) for Mg-vermiculite. Contours for octahedral ( $C$ ) atoms at intervals of  $4e \cdot \text{Å}^{-2}$ , for tetrahedral ( $D$ ) atoms and oxygens  $2e \cdot \text{Å}^{-2}$ , for  $\text{H}_2\text{O}$  and exchangeable  $\text{Mg}^{2+}$  at  $1e \cdot \text{Å}^{-2}$ . The dotted line represents the  $1e \cdot \text{Å}^{-2}$  level. Distances parallel to the  $z$ -axis are indicated at the right-hand side of the diagram.

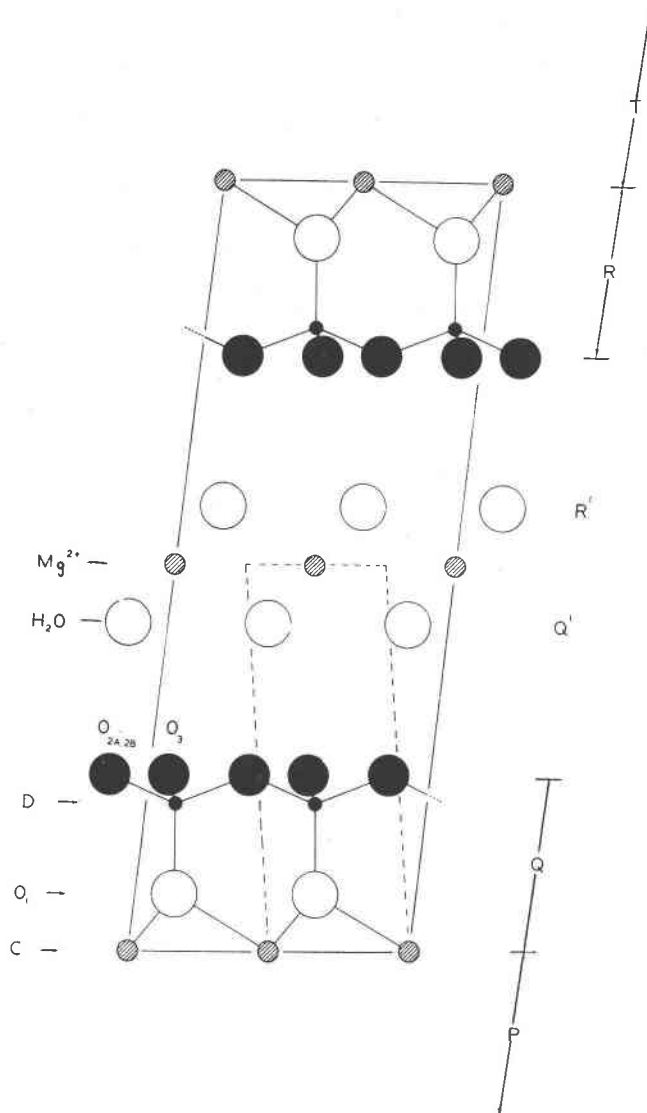


FIG. 1. (b) The corresponding crystal structure of Mg-vermiculite projected on (010). *P*, *Q*, *R* and *T* refer to silicate half-layers; *Q'* and *R'*, sheets of water molecules; *C*, (Mg, Fe, Al) octahedrally-coordinated atoms; *D*, (Al, Si) tetrahedrally-coordinated atoms; *O*<sub>1</sub>, oxygens and hydroxyls at  $z=0.037$ ; *O*<sub>2A</sub>, *O*<sub>2B</sub>, *O*<sub>3</sub>, oxygens at  $z=0.114$ ; H<sub>2</sub>O, interlamellar water molecules; Mg<sup>2+</sup>, interlamellar cations. An area,  $(a/2) \times (c/4)$ , of the unit cell selected by Hendricks and Jefferson (1938*a*) is indicated by the broken lines.

(i.e.,  $c = 28.90 \text{ \AA}$ ). The general reflexions,  $hkl$ , occur only for  $h+k=2n$ . The space group for the structure, based on this value of  $\beta$ , is  $Cc$  or  $C2/c$ . If the value  $\beta = 93.5^\circ$  is used, the  $k=3n$  spectra are accounted for by a cell centered on all faces and containing two silicate layers. The correct space group for this unit cell is either  $Cn$  or  $C2/n$ , not  $Cc$  or  $C2/c$  as reported by Hendricks and Jefferson (1938a). The relation of their unit cell to the one selected in the present study is shown in Fig. 1b.

Intensity data for the  $00l$ ,  $h0l$  and  $h3l$  reflexions were recorded on the Weissenberg goniometer using filtered Mo radiation. For each set of reflexions, two packs, each of four films interleaved with tin-foil to increase the inter-film ratio, were exposed for 100 and 5 hours respectively. Intensity estimations were made by comparison with a set of standards obtained by timed exposures of a selected individual reflexion oscillated over a small angular range. For the diffuse reflexions, a crystal was chosen which gave some indication of diffraction maxima rather than the very diffuse streaks produced by most specimens. Filtered Cu radiation was utilised to provide adequate resolution of the peaks. The distribution of the  $02l$  reflexions was measured by means of a Leeds-Northrop recording microphotometer and corrected for film background (Fig. 2).

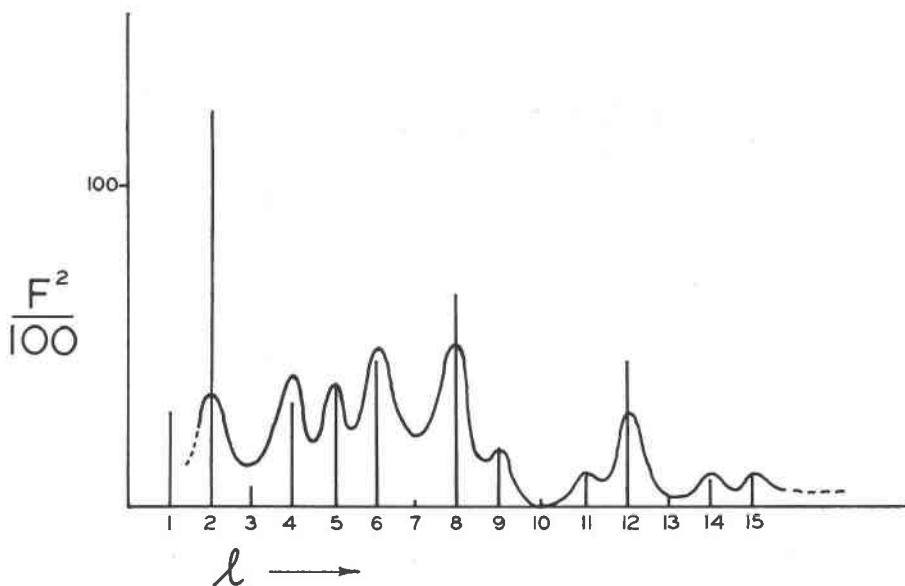


FIG. 2. Photometer curve of the  $02l$  diffuse reflexions, corrected for film background. The calculated values for the mean-positional arrangement of structures  $q$  and  $r$  are superimposed for comparison.

The  $F^2$  values of the  $00l$ ,  $h0l$  and  $h3l$  reflexions were obtained after correction for polarization and Lorentz factors by graphical means (Kaan and Cole, 1949). The structure amplitudes were later placed on an approximately absolute scale by correlation with the calculated values. For the calculation of structure amplitudes, the scattering factors for  $Mg^{2+}$  and  $Si^{4+}$  (Internationale Tabellen, 1935) were loaded by the respective isomorphous replacements indicated by the formula based on a chemical analysis of the sample (Table 1). The temperature factor,  $B=1.2 \times 10^{-16}$  cm.<sup>2</sup>, was determined by plotting  $\log \Sigma |F_c| / \Sigma |F_o|$  against  $\sin^2 \theta$  in six equal ranges of  $\sin^2 \theta$  from 0.0 to 0.6 (Wilson, 1942). Fourier summations were carried out on three-figure Beevers-Lipson strips, the  $a$  and  $c$  axes being subdivided into 30 and 120 parts respectively. The electron-density map was drawn from contour values derived from interpolated sections.

Because of the frequent association of chlorite and vermiculite as mixed-layer structures, it was necessary to be certain that the specimen under investigation contained no interleaved chloritic material, although previous examination of the total sample had indicated its purity. The crystal from which the  $h0l$  and  $h3l$  data had been obtained was therefore converted to Li-vermiculite, and the  $00l$  reflexions rephotographed. A prolonged exposure showed the characteristic 12.2 Å basal reflexion of Li-vermiculite with a regular series of higher orders (Milne and Walker, *loc. cit.*). No sign of a 14 Å reflexion, such as would be produced by the presence of chlorite, could be found. On this basis, it is estimated that the specimen contained less than 0.5 per cent of chlorite layers.

#### STRUCTURE ANALYSIS

Initial attempts at a unidimensional synthesis of this vermiculite were reported by Milne and Walker (1951), and an interim statement of results in the present investigation was made in 1952 (Mathieson and Walker).

##### 1. *Electron-density distribution normal to (001)*

For the preliminary synthesis, the signs of the  $00l$  structure amplitudes of Mg-vermiculite recorded up to the 62nd order were computed from the contributions of the atoms of the silicate layer alone. Omission of the water molecules and exchangeable cations from the calculations ensured that no assumptions would be involved in their location. Apart from the distribution corresponding to the silicate layer, the synthesis disclosed two additional peaks, one at  $z=0.214$  and a smaller one at  $z=0.250$ .

A unidimensional synthesis of the same crystal after conversion to

Sr-vermiculite reproduced the electron-density curve of the Mg-vermiculite except for the peak at  $z=0.25$ , which was substantially increased in size. The exchangeable cations are therefore located midway between the silicate layers. The water molecules are arranged on either side of the central cations in sheets which lie at a distance of 2.83 Å from the surface oxygens of the adjacent silicate layers.

Recalculation of the structure amplitudes, taking into account the contributions of the water molecules and exchangeable cations, gave reliability factors,

$$R = \frac{\sum |F_o - F_c|}{\sum |F_o|},$$

of 0.14 and 0.22 for Mg- and Sr-vermiculite respectively (Table 2).

### 2. Projection along the *b*-axis

Since the approximate configuration of the silicate layer is known, this portion of the structure can be disposed in the unit cell by consideration of the structure amplitudes for the reflexions 20,12 to 20 $\bar{4}$  (see Table 2). With the approximate  $x$  parameters derived by this means and taking the  $z$  parameters from the line synthesis, a preliminary set of structure amplitudes for the  $h0l$  reflexions was calculated. Again the contributions of the water molecules and exchangeable cations were omitted initially so that no assumptions would be involved in their location. The resultant electron-density contour map provided more accurate parameters for the atoms of the silicate layer, and located the water molecules at  $x=0.142$ ,  $z=0.213$  and the exchangeable cations at  $x=0.0$ ,  $z=0.250$ . Recalculation of the structure amplitudes for all constituents of the unit cell necessitated changes in sign for a few minor terms only, and a subsequent synthesis produced the electron-density distribution shown in Fig. 1*a*. The corresponding diagram of the crystal structure is given in Fig. 1*b*. The final reliability factor for  $h0l$  reflexions was 0.15.

### 3. The Crystal Structure in Three Dimensions

Initially, deductions arising from the sharp  $k=3n$  spectra will be considered and the results referred to a sub-cell containing a single silicate layer ( $c=14.45$  Å).

From the equivalence of the [010], [310] and [ $\bar{3}10$ ] axes, it is evident that the projections of the crystal structure along [310] and [ $\bar{3}10$ ] will be identical with that along [010] (Fig. 1*b*). The three projections can therefore be combined to give the complete structure if the coordination values of the atoms are also taken into account. The crystal structure of half a silicate layer (e.g., Q, Fig. 1*b*) viewed normal to (001) is shown

TABLE 2. COMPARISON OF OBSERVED AND CALCULATED STRUCTURE AMPLITUDES FOR (a) Sr-VERMICULITE AND (b) Mg-VERMICULITE. NOTE THAT  $F(20l) = F(13, l+2)$ : SLIGHT DIFFERENCES IN THE CALCULATED VALUES FOR THESE SETS OF REFLEXIONS ARE DUE TO APPROXIMATIONS IN THE ATOMIC PARAMETERS AND SCATTERING FACTORS

(a)			(b)								
00l	$F_{obs.}$	$F_{calc.}$	00l	$F_{obs.}$	$F_{calc.}$	h0l	$F_{obs.}$	$F_{calc.}$	h0l	$F_{obs.}$	$F_{calc.}$
002	—	298	002	282	305	20,58	<25	6	20,5 $\bar{6}$	<23	-13
004	—	78	004	62	39	20,56	<24	21	20,5 $\bar{8}$	<24	5
006	—	-93	006	110	-72	20,54	<23	20	20,6 $\bar{0}$	<25	3
008	219	168	008	211	213	20,52	<22	6	20,6 $\bar{2}$	<27	11
00,10	344	336	00,10	342	313	20,50	<22	-1			
00,12	55	21	00,12	60	-67	20,48	<21	-12	40,52	<26	-18
00,14	185	-114	00,14	105	-79	20,46	<20	14	40,50	<26	-8
00,16	63	-76	00,16	74	-95	20,44	37	28	40,48	29	33
00,18	<20	4	00,18	86	124	20,42	32	39	40,46	46	45
00,20	209	224	00,20	167	161	20,40	<19	17	40,44	23	38
00,22	66	69	00,22	84	91	20,38	<18	-9	40,42	<24	-9
00,24	150	150	00,24	121	121	20,36	68	70	40,40	<23	27
00,26	52	41	00,26	42	34	20,34	100	92	40,38	46	44
00,28	54	88	00,28	83	110	20,32	105	122	40,36	63	59
00,30	65	85	00,30	68	69	20,30	16	6	40,34	35	18
00,32	76	87	00,32	107	108	20,28	16	-20	40,32	<20	-22
00,34	94	95	00,34	61	61	20,26	16	31	40,30	<20	0
00,36	64	44	00,36	<20	2	20,24	105	87	40,28	<19	8
00,38	39	-30	00,38	38	-19	20,22	79	109	40,26	52	53
00,40	<26	-9	00,40	<22	-11	20,20	37	-57	40,24	52	42
00,42	<27	-13	00,42	41	59	20,18	63	-48	40,22	29	35
00,44	61	76	00,44	39	33	20,16	37	23	40,20	29	42
			00,46	<24	-7	20,14	173	173	40,18	46	26
			00,48	<24	-11	20,12	263	257	40,16	150	142
			00,50	<25	20	20,10	105	87	40,14	162	143
			00,52	54	76	208	178	189	40,12	144	152
			00,54	39	33	206	116	81	40,10	<16	-8
			00,56	<26	9	204	304	300	408	16	-33
			00,58	<26	-7	202	205	212	406	63	81
			00,60	<27	9	200	136	127	404	167	134
			00,62	27	23	202	16	20	402	58	94
						20 $\bar{4}$	147	173	400	110	-126
						20 $\bar{6}$	32	51	40 $\bar{2}$	87	-69
						20 $\bar{8}$	100	72	40 $\bar{4}$	127	122
						20,1 $\bar{0}$	147	175	40 $\bar{6}$	225	223
						20,1 $\bar{2}$	58	41	40 $\bar{8}$	167	178
						20,1 $\bar{4}$	47	-40	40,1 $\bar{0}$	<16	-30
						20,1 $\bar{6}$	152	163	40,1 $\bar{2}$	58	73
						20,1 $\bar{8}$	236	203	40,1 $\bar{4}$	127	132
						20,2 $\bar{0}$	294	281	40,1 $\bar{6}$	196	206
						20,2 $\bar{2}$	63	37	40,1 $\bar{8}$	75	77

TABLE 2—(continued)

(b)

00l	$F_{obs.}$	$F_{calc.}$	00l	$F_{obs.}$	$F_{calc.}$	h0l	$F_{obs.}$	$F_{calc.}$	h0l	$F_{obs.}$	$F_{calc.}$
						20,24	<16	1	40,20	<18	-23
						20,26	16	30	40,22	29	-7
						20,28	105	100	40,24	<18	9
						20,30	89	98	40,26	52	61
						20,32	<17	-24	40,28	58	31
						20,34	52	-30	40,30	17	26
						20,36	<18	-11	40,32	<20	18
						20,38	37	57	40,34	<20	13
						20,40	73	70	40,36	63	68
						20,42	37	25	40,38	81	66
						20,44	26	31	40,40	81	76
						20,46	<20	11	40,42	<22	8
						20,48	47	54	40,44	<23	-5
						20,50	47	36	40,46	<23	17
						20,52	37	28	40,48	40	32
						20,54	<22	7	40,50	<24	27

h0l	$F_{obs.}$	$F_{calc.}$	h0l	$F_{obs.}$	$F_{calc.}$	h0l	$F_{obs.}$	$F_{calc.}$	h3l	$F_{obs.}$	$F_{calc.}$
40,52	<25	-24	80,20	<23	5	12,08	47	24	13,46	47	53
40,54	<25	-18	80,18	<23	19	12,0,10	<30	14	13,44	<27	11
40,56	<26	8	80,16	<22	4	12,0,12	<30	1	13,42	21	30
40,58	23	29	80,14	<22	-9	12,0,14	<30	2	13,40	28	23
40,60	<27	22	80,12	<22	-2	12,0,16	<30	11	13,38	68	67
			80,10	42	30	12,0,18	<30	10	13,36	46	55
60,42	<23	-7	808	79	70				13,34	26	-12
60,40	<23	-7	806	37	42				13,32	17	-28
60,38	<22	30	804	<21	20				13,30	48	-24
60,36	<22	12	802	<21	4				13,28	88	97
60,34	<21	-10	800	63	54				13,26	98	96
60,32	<20	-26	802	74	74				13,24	15	27
60,30	20	19	804	32	31				13,22	<23	2
60,28	76	72	806	26	-24				13,20	62	38
60,26	50	51	808	16	-32				13,18	209	271
60,24	<19	27	80,10	<20	27				13,16	204	196
60,22	<19	-5	80,12	48	51				13,14	139	157
60,20	50	57	80,14	<20	19				13,12	45	-40
60,18	81	77	80,16	<20	-6				13,10	49	40
60,16	66	55	80,18	<21	2				138	171	180
60,14	<18	-2	80,20	37	56				136	120	74
60,12	35	-34	80,22	63	60				134	32	49
60,10	<17	14	80,24	58	47				132	206	169

TABLE 2—(continued)

$h0l$	$F_{obs.}$	$F_{calc.}$	$h0l$	$F_{obs.}$	$F_{calc.}$	$h0l$	$F_{obs.}$	$F_{calc.}$	$h3l$	$F_{obs.}$	$F_{calc.}$
608	45	35	80,26	<22	17				130	<20	18
606	60	56	80,28	<22	3				132	141	130
604	35	36	80,30	<22	18				134	234	210
602	<17	10	80,32	<22	13				136	313	298
600	35	43	80,34	<23	17				138	141	82
602	71	62	80,36	<23	0				13,10	174	187
604	141	142	80,38	<23	-7				13,12	113	92
606	96	91	80,40	<24	-7				13,14	227	259
608	35	43	80,42	<24	7				13,16	179	171
60,10	20	-18	80,44	<25	32				13,18	32	24
60,12	<18	21	80,46	<25	19				13,20	49	-45
60,14	76	90	80,48	<26	13				13,22	45	-58
60,16	66	54							13,24	76	109
60,18	<19	-11	10,0,14	<26	21				13,26	95	89
60,20	50	-57	10,0,12	47	37				13,28	21	30
60,22	<19	12	10,0,10	26	24				13,30	<23	-19
60,24	86	94	10,08	<25	13				13,32	<24	6
60,26	81	75	10,06	<24	14				13,34	101	123
60,28	30	34	10,04	<24	9				13,36	112	92
60,30	<20	-9	10,02	<23	16				13,38	63	69
60,32	30	52	10,00	<23	6				13,40	<25	-8
60,34	60	67	10,02	<23	6				13,42	<26	15
60,36	55	53	10,04	<22	0				13,44	29	39
60,38	<21	7	10,06	<22	-8				13,46	30	28
60,40	<21	-15	10,08	<22	10				13,48	<28	13
60,42	<22	7	10,0,10	36	28						
60,44	<22	9	10,0,12	42	43				33,40	<28	36
60,46	<23	14	10,0,14	<23	15				33,38	<27	12
60,48	<24	3	10,0,16	<23	5				33,36	<27	-3
60,50	<24	0	10,0,18	<24	18				33,34	<26	-24
60,52	<25	10	10,0,20	36	41				33,32	23	21
60,54	<26	11	10,0,22	26	32				33,30	78	91
			10,0,24	<25	-7				33,28	68	78
80,32	<27	34	10,0,26	<25	-21				33,26	51	60
80,30	<26	30	10,0,28	<26	0				33,24	<24	-16
80,28	<25	27	10,0,30	<26	19				33,22	73	75
80,26	<25	11	10,0,32	<27	15				33,20	132	115
80,24	<24	-1							33,18	136	119
80,22	<24	12	12,06	<30	19				33,16	<23	19

TABLE 2—(continued)

$hkl$	$F_{obs.}$	$F_{calc.}$	$hkl$	$F_{obs.}$	$F_{calc.}$	02l	$F_{calc.}$	$\frac{F^2 calc.}{100}$
33,14	70	82	53,30	44	41	021	54	29
33,12	<22	7	53,32	46	70	022	111	123
33,10	90	60	53,34	<28	-9	023	-25	6
338	139	134	53,36	<29	-25	024	56	31
336	65	50	53,38	<29	-19	025	-61	37
334	<22	-8	53,40	<30	45	026	-67	45
332	107	104	53,42	<30	58	027	-11	1
330	207	140				028	-81	66
332	315	304	73,20	<28	13	029	43	18
334	175	140	73,18	<27	1	02,10	10	1
336	82	102	73,16	<26	26	02,11	30	9
338	<22	-5	73,14	76	79	02,12	67	45
33,10	58	53	73,12	76	73	02,13	-15	2
33,12	116	143	73,10	34	37	02,14	29	8
33,14	84	59	738	<25	-1	02,15	-31	10
33,16	-23	4	736	<25	9			
33,18	62	-88	734	45	50			
33,20	<23	24	732	56	38			
33,22	130	135	730	<25	20			
33,24	117	122	732	<25	-35			
33,26	62	79	734	<25	-4			
33,28	<24	-15	736	50	41			
33,30	36	71	738	78	72			
33,32	68	89	73,10	62	68			
33,34	78	99	73,12	<25	18			
33,36	23	24	73,14	<25	27			
33,38	<25	-30	73,16	<26	45			
33,40	<26	0	73,18	64	72			
33,42	<26	16	73,20	56	55			
33,44	<27	33	73,22	<26	-2			
33,46	<27	4	73,24	<27	-13			
			73,26	<28	-12			
			73,28	34	36			
53,32	55	58	73,30	34	29			
53,30	54	71	73,32	<30	11			
53,28	<26	23	73,34	<32	-6			
53,26	<25	-15						
53,24	<25	13						
53,22	43	39	936	<28	22			
53,20	67	72	934	<28	30			
53,18	<24	-21	932	<27	8			
53,16	40	-35	930	<27	-5			
53,14	<24	-4	932	<26	21			
53,12	109	102	934	53	47			
53,10	135	133	936	53	56			

TABLE 2—(continued)

$h3l$	$F_{obs.}$	$F_{calc.}$	$h3l$	$F_{obs.}$	$F_{calc.}$	02l	$F_{calc.}$	$\frac{F^2 calc.}{100}$
538	52	51	938	<25	31			
536	<24	27	93, $\bar{1}0$	<25	-1			
534	43	40	93, $\bar{1}2$	<25	-12			
532	143	134	93, $\bar{1}4$	<25	-3			
530	142	130	93, $\bar{1}6$	<25	7			
532	49	34	93, $\bar{1}8$	39	25			
534	<24	-4	93, $\bar{2}0$	<26	31			
536	43	-47	93, $\bar{2}2$	<27	12			
538	43	58	93, $\bar{2}4$	<28	10			
53, $\bar{1}0$	68	53						
53, $\bar{1}2$	58	70						
53, $\bar{1}4$	<24	16						
53, $\bar{1}6$	<25	4						
53, $\bar{1}8$	47	64						
53, $\bar{2}0$	96	102						
53, $\bar{2}2$	111	127						
53, $\bar{2}4$	50	35						
53, $\bar{2}6$	<26	-2						
53, $\bar{2}8$	<27	13						

in Fig. 3a. On the basis of the diffraction data considered so far, the arrangement of the water molecule sites and the exchangeable cation sites ( $m_1, m_2, m_3$ ) can be represented diagrammatically by the view (normal to (001) and projected on the base of the cell) of the layer  $Q'R'$  (Fig. 3b). The chemical data indicate that the water molecule and exchangeable cation sites are approximately two-thirds and one-ninth filled respectively. Calculation of the  $h3l$  structure amplitudes for this structure gives satisfactory agreement with the observed values (Table 2) establishing its essential correctness ( $R=0.17$ ). Table 3 lists the atomic coordinates; the alternative sets of values ( $a$ ) and ( $b$ ), given for the  $x$  and  $y$  coordinates of the water molecule sites, will be discussed at a later stage.

The structure of the silicate layer which emerges is very similar to that put forward by previous workers, although greater detail is revealed than has hitherto been obtained for layer silicate structures, largely because of increased precision of intensity estimation combined with refinement by successive Fourier syntheses. The bond lengths are as

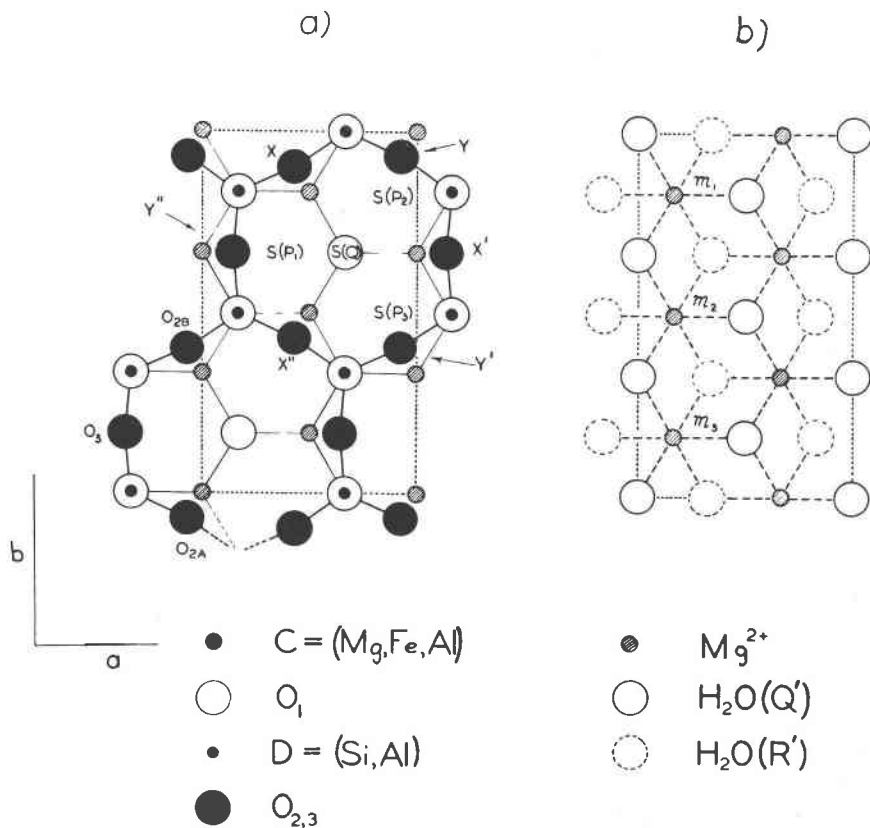


FIG. 3. (a) Section of the crystal structure of Mg-vermiculite from  $z=0.0$  to  $0.114$  (i.e. half-layer  $Q$ ) projected on the base of the cell normal to  $(001)$ . (b) Section of the crystal structure from  $z=0.213$  to  $0.287$ , i.e., sites of the water molecules in sheets  $Q'$  and  $R'$  and sites of exchangeable  $Mg^{2+}$  cations.

follows:  $C^*-O_1$ ,  $2.06 \text{ \AA}$ ;  $D^*-O_1$ ,  $1.69 \text{ \AA}$ ; and  $D-O_{2A}$ ,  $D-O_{2B}$ ,  $D-O_3$ ,  $1.62 \text{ \AA}$  each (probable error,  $\pm 0.02 \text{ \AA}$ ). The oxygen atom  $O_1$  is linked tetrahedrally with one  $D$  (or hydrogen) and three  $C$  atoms, the angle  $COD$  being  $109^\circ$ , whereas  $O_{2A}$ ,  $O_{2B}$  and  $O_3$  are each linked to two  $D$  atoms with a  $DOD$  angle of  $142^\circ$ . If  $r(Si^{4+})$  is taken as  $0.41 \text{ \AA}$ , then  $r(O_1)$  is  $1.28 \text{ \AA}$  and  $r(O_2, O_3)$ ,  $1.21 \text{ \AA}$ . The relationship between ionic radius and coordination number (Wells, 1950, p. 71) gives the ratio of two-

\* For convenience,  $C$  will be used to represent the (Mg, Fe, Al) atoms in octahedral positions at the centre of the silicate layer; and  $D$ , the (Si, Al) tetrahedrally-coordinated atoms near the surface. The key to the oxygen atoms is given in Figs. 1b and 3a.

four-coordinated radii as  $(2/4)^{\frac{1}{2}} = 0.92$  and the observed ratio, 0.95, is therefore of the correct order.

The contour map clearly indicates a distortion in the surface oxygen sheet of the silicate layer. The hexagon of oxygen atoms  $XYX'Y'X''Y''$  (Fig. 3a) is not regular but consists of two interpenetrating isosceles triangles of oxygens  $XX'X''$  and  $YY'Y''$  with sides 4.35 and 4.84 Å respectively. The corresponding distance in a regular hexagon would be 4.59 Å. The distortion is accounted for by a rotation through  $5\frac{1}{2}^\circ$  of the triad of oxygens above each *D* atom. Since the change from the ideal hexagonal to the distorted configuration would involve differences in *D*-O bond lengths of less than 0.01 Å, it is improbable that the distortion arises from inability to accommodate a regular hexagonal oxygen network in the cross-sectional area of the unit cell (i.e.,  $9.18 \times 5.33$  Å). The distortion is more readily explained on the basis of electrostatic forces within the silicate layer, if it is assumed that a residual negative charge on each surface oxygen interacts with a residual positive charge on the octahedral *C* atom lying below and to one side (viewed normal to (001)). The electrostatic forces thus invoked are correctly disposed to produce a torque in the required direction (Fig. 3a), the angular movement being limited by the over-riding factor of the *D*-O distance.

At this juncture, it is appropriate to consider the approximate spatial relationships of the interlamellar water and exchangeable cation sites to an adjacent silicate layer. It will be assumed for the moment that the water molecules all lie at the centre of the peak of the electron-density distribution (Fig. 1a), although the possibility that this is merely a mean position will be suggested later. The sites for the water molecules lie directly over *C* atoms and those for the exchangeable cations over *D* atoms (or hydroxyls) of the silicate layer. This latter observation indicates an important point with regard to the relationship of adjacent silicate layers, namely the collinearity of (i) atoms  $O_1$  and *D* (or *H*) of the half-layer *Q*, (ii) the exchangeable cation site, and (iii) atoms *D* (or *H*) and  $O_1$  of the half-layer *R* (Fig. 1b).

The structure of complete silicate layers and the method of stacking of the layers can be deduced from a consideration of the  $k \pm 3n$  spectra. The water molecules and exchangeable cations were omitted from the calculations since they can only have a minor influence on the structure amplitudes. The  $02l$  reflexions were employed in testing the various possible structures.

In discussing the silicate layers, it is convenient to focus attention on the site at the centre of the distorted hexagon of surface oxygen atoms. Let this site be  $S(Z)$  where *Z* refers to the half-layer *P*, *Q*, *R* or *T*. Then the half-layers *P* and *Q* combine to form a single layer and  $S(Q)$  can be associated with  $S(P_1)$ ,  $S(P_2)$  or  $S(P_3)$  (Fig. 3a). These three possible

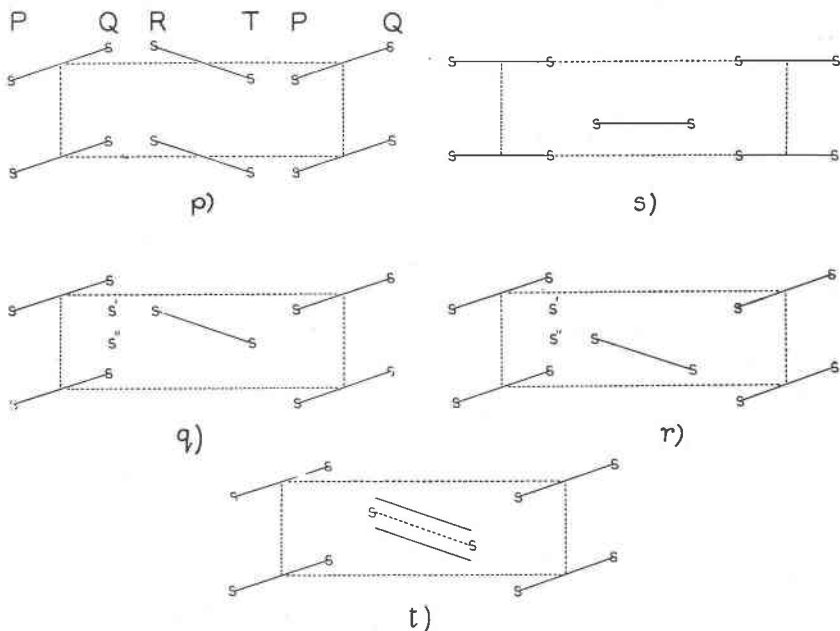


FIG. 4. Schematic presentation of the possible stacking sequences in Mg-vermiculite. (*p*) (*q*) and (*r*) *N*-type silicate layer displaced with respect to an *M*-type layer by 0,  $b/3$  and  $2b/3$  respectively. (*s*) *L*-type layers displaced by  $b/3$  (or  $2b/3$ ). (*t*) Positional mean of structures *q* and *r*.

layer structures correspond to the *L*, *M* and *N* types of layers referred to by Brindley, Oughton and Robinson (1950) in their study of the chlorites. The three types of silicate layer have individual symmetry  $C2/m$  and are indistinguishable until the *b* axis of the crystal is defined by the mutual relations of the stacked layers. When a second complete silicate layer *RT* is added, there are twelve possible ways of grouping *P*, *Q*, *R* and *T*. The existence of a glide operation *c* reduces the possibilities to four, illustrated diagrammatically in Fig. 4 *p*, *q*, *r* and *s*. As Hendricks and Jefferson (1938*a*) have shown, none of these arrangements yields structure amplitudes in agreement with the observed intensity distribution. However, structures *q* and *r* give some measure of agreement for reflections  $02l$  where  $l=2n$ , and a structure with the unit *RT* located at the centre of the projection area (Fig. 4 *t*) gives a very close agreement with the observed distribution of intensities for the  $02l$  spectra. Table 2 lists the amplitudes calculated for this arrangement, and Fig. 2 shows the  $F^2$  values superimposed on the photometer curve.

The solution obtained in this way is completely contrary to all the evidence of the sub-cell analysis, according to which the site *S*(*R*) should

lie over the site  $S(Q)$  or displaced therefrom by  $\pm b/6$  in this projection (i.e.,  $S'$  or  $S''$ , Fig. 4). Furthermore, a unique structure for vermiculite would be implied by structure  $t$  and therefore no explanation for the occurrence of the diffuse spectra would be possible. The deductions from both the sharp and diffuse spectra can be reconciled only if it is assumed that structures  $q$  and  $r$  are equally probable and that structure  $p$  does not occur. In other words, the stacking of the silicate layers in vermiculite corresponds to  $M$ -type layers alternating with  $N$ -type layers. The layers, however, can only be arranged so that site  $S(R)$  is not in line with site  $S(Q)$  nor  $S(P)$  with  $S(T)$ . The resultant crystal structure can be represented for the purposes of calculation by the average structure  $t$  (Fig. 4). The mutual relationships of the surface oxygens of the silicate half-layers  $Q$  and  $R$  are illustrated in Fig. 5.

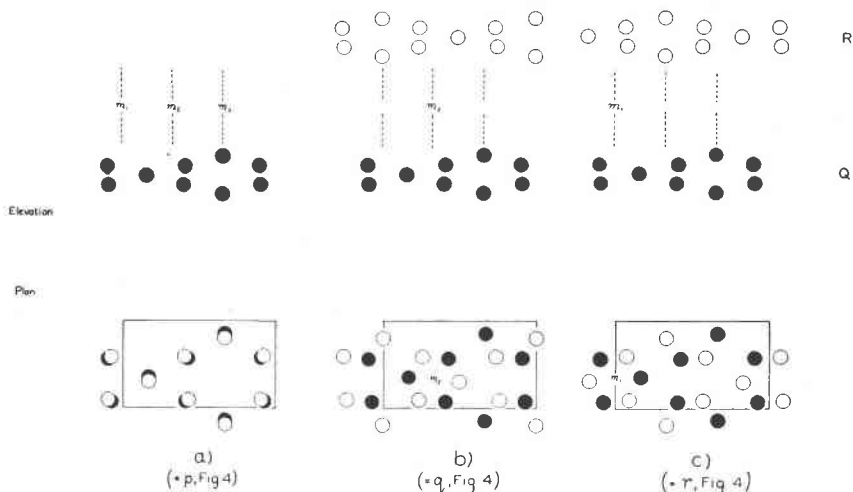


FIG. 5. Plan and elevation of the relationship between the surface oxygen network of half-layers  $Q$  and  $R$ .  $m_1, m_2, m_3$  are sites for exchangeable cations as deduced from the sub-cell analysis, and are defined by their relationship to the half-layer  $Q$ . Projections are normal to (001).

#### 4. Location of the Sites of the Water Molecules

In the  $b$ -axis projection (Fig. 1a), the contours of the water molecules tend to be drawn out parallel to the  $a$  axis and there is evidence of a tail in the negative  $x$ -direction. As a result, the peak height is lower than would be expected for 2.16 water molecules (Table 1).

At first sight, the shape of the water peak might seem to be due to high thermal energy in the water molecules, producing movement mainly parallel to (001) because of restrictions imposed by the environment.

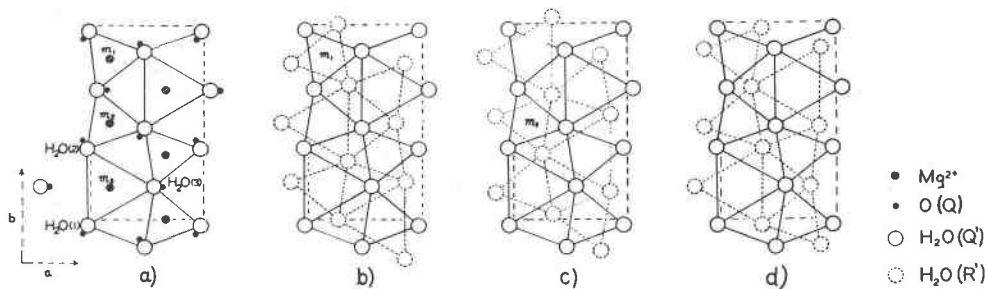


FIG. 6. (a) Diagram of the relation of the distorted water network  $Q'$  to the surface oxygen network of the half-layer  $Q$ . Cation sites  $m_1$ ,  $m_2$ ,  $m_3$  are also shown. This diagram illustrates the tendency of each water molecule to approach more closely to its associated surface oxygen. (b), (c), (d) The three ways of combining two sheets of water sites, the relative shifts being  $b/3$ ,  $2b/3$  and 0 respectively. (d) is excluded by the data. The sites  $m_1$  and  $m_2$  with suitable undistorted octahedral environment for the  $Mg^{2+}$  cations are shown.

This explanation, however, does not account for the "tail" on the water molecule peak and, in order to do so, it must be assumed that the asymmetric electron-density distribution corresponds to regular displacements of the water molecules from the mean position (Table 3, column (a)). In this event, one would expect such displacements to be related to the adjacent oxygen network and, in a triad of water molecules ( $H_2O(1)$ ,  $H_2O(2)$ ,  $H_2O(3)$ , Fig. 6a) over a surface oxygen hexagon, each member of the triad would be displaced equally towards or away from its related oxygen, i.e., the triad would expand or contract. If it expands, there must be concomitant rotations of unexpanded triads in opposite directions around  $m_1$  and  $m_2$  (Fig. 6a), and the corresponding electron-density distribution viewed along the  $b$ -axis would develop a tail in the negative  $x$ -direction such as is indicated in the contour map (Fig. 1a)\*. The distortion of the water sheet produced in this way results in a closer approach of each water molecule to its related oxygen atom. The relevant atomic parameters are listed in column (b), Table 3.

Since each water sheet is located by its relation to the adjacent silicate layer surface, a complete water layer (consisting of two sheets of water molecules) can only be formed by superimposing the water sheets in the two ways permitted by the stacking of the silicate layers. These two arrangements correspond to relative shifts of  $b/3$  and  $2b/3$ , and are illustrated in Fig. 6 b and c respectively. Inspection shows that the two arrangements are equivalent and, in both, the relative displacements of the water molecules maintain normal  $H_2O-H_2O$  approach distances be-

\* The displacement of the water molecules from their ideal hexagonal positions cannot be determined accurately from the shape of the electron-density distribution but is probably of the order of 0.2 Å.

TABLE 3. ATOMIC PARAMETERS FOR MG-VERMICULITE

Atom		x		y		z
	C	0		0		0
	C	0		0.333		0
	C	0		0.667		0
	O <sub>1</sub>	0.358		0		0.037
	O <sub>1</sub>	0.358		0.333		0.037
	O <sub>1</sub>	0.358		0.667		0.037
	D	0.397		0		0.096
	D	0.397		0.333		0.096
	O <sub>2A</sub>	0.147		0.404		0.114
	O <sub>2B</sub>	0.147		0.929		0.114
	O <sub>3</sub>	0.434		0.167		0.114
		(a)	(b)	(a)	(b)	
H <sub>2</sub> O	site (1)	0.142	0.160	0	-0.019	0.213
	site (2)	0.142	0.160	0.333	0.352	0.213
	site (3)	0.142	0.105	0.667	0.667	0.213
Mg <sup>2+</sup>	site m <sub>1</sub>	0.500		0		0.250
	site m <sub>2</sub>	0.500		0.333		0.250
	site m <sub>3</sub>	0.500		0.667		0.250

tween the sheets. The method of stacking the water sheets illustrated in Fig. 6 *d* is excluded, since it could only exist if structure *p* (Fig. 4) were permissible. The nonoccurrence of structure *p* is perhaps connected with the fact that such a water-layer arrangement would involve very close approach of the water molecules between the sheets.

### 5. The Structure of the Interlamellar Region

From the previous sections, it is evident that the arrangement of the *sites* of the interlamellar cations and water molecules closely resembles that of the octahedral *C* atoms and *O*<sub>1</sub> atoms, respectively, of the silicate layers although, in the former, the water sites are displaced somewhat from the regular octahedral arrangement. According to the chemical data, however, only a proportion of the interlamellar water and cation sites are occupied at one time.

Since each water site is equivalent with respect to the associated oxygen of the silicate layer surface, any grouping of the water molecules will be due to the influence of the cations. The importance of the cations in this respect is suggested by the variation of the interlamellar spacing produced when other cations are substituted for the Mg (Milne and Walker, 1950). A certain amount of evidence has been adduced by others to show that Mg ions tend to attract octahedral hydration shells in

water solution (e.g. Bernal and Fowler, 1933), and such octahedral grouping is known to occur in crystal hydrates such as magnesium chlorate hexahydrate (West, 1935). It is reasonable to suppose, therefore, that there will be a tendency for the exchangeable Mg ions in vermiculite to form hydration shells.

Examination of the two equivalent water-layer structures in Fig. 6 *b* and *c* reveals that in each case only one of the three  $m$  cation sites provides *undistorted* octahedral coordination for a cation ( $m_1$  in Fig. 6 *b* or  $m_2$  in Fig. 6 *c*). The  $\text{Mg}^{2+}-\text{H}_2\text{O}$  distance of 2.06 Å involved, moreover, is in agreement with that observed in magnesium benzene sulphonate hexahydrate (Broomhead and Nicol, 1948) which is the most accurate value available. All other sites have an asymmetric environment of water molecules, consisting of an unexpanded triad in one sheet and an expanded triad in the other. Equal  $\text{Mg}^{2+}-\text{H}_2\text{O}$  distances at these sites could only be maintained by displacing the cations 0.06 Å from the central plane, which is beyond the limit of error of measurement from the contour map (Fig. 1*a*). The resultant equilibrium  $\text{Mg}^{2+}-\text{H}_2\text{O}$  distance, moreover, would be 2.20 Å. It is almost certainly true, therefore, that the cations will occupy  $m_1$  or  $m_2$  sites depending on the stacking of the adjacent silicate layers.

The degree of ordering of the water molecules and cations within the available sites can now be considered further. The possibility of order *within an individual water-cation layer* is not excluded by the diffraction data since mutual ordering of these layers would be necessary for their structure to be revealed by the data. A case for the existence of long-range order of this nature, not directly deducible from the diffraction evidence, has been convincingly put forward in recent studies of hollandite (Byström, 1951) and psilomelane (Wadsley, 1952). So far, we have shown that the exchangeable cations in vermiculite lie in a plane midway between adjacent silicate layers, and that their lateral disposition is related to the adjacent water sheets. There are, however, only enough cations to fill one in three of the available  $m_1$  (or  $m_2$ ) sites.

If it is assumed that the cations, due to mutual repulsion effects, tend to distribute themselves uniformly throughout the available sites, a hexagonal distribution of the type shown in Fig. 7 is obtained. Six water molecules can be arranged around and in contact with a Mg ion at a  $u$  site, a triad in the upper and a triad in the lower sheet, forming the single hydration shell already postulated. In the lower sheet, additional waters can be added in groups of three around unoccupied sites  $v$  or  $w$ . The water molecule sites around  $w$  in this sheet will be closer to the cations than those around  $v$ , so that the former sites will be preferred if it is assumed that the tendency of the cations to form single hydration

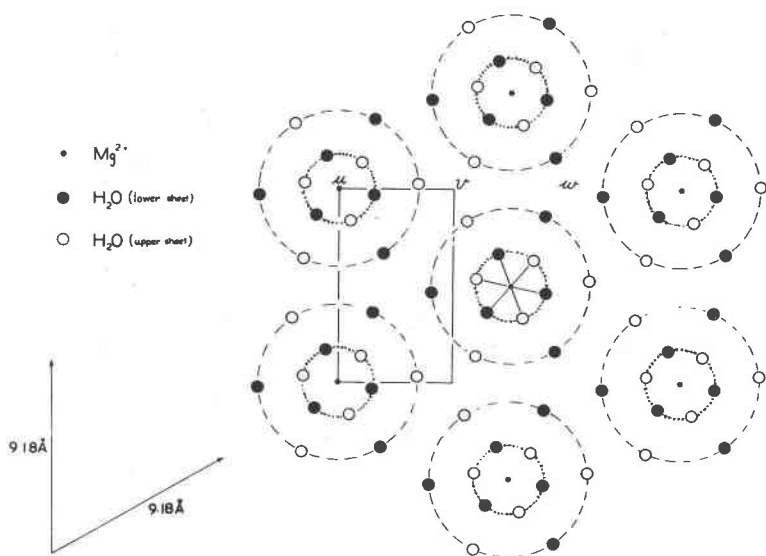


FIG. 7. Diagram of the proposed structure of the interlamellar region. Sites  $u$ ,  $v$ ,  $w$ , are all of type  $m_1$  (or all of type  $m_2$ ).

shells indicates a similar although less-marked tendency to form second shells.\* In the upper sheet, sites around  $v$  will be preferred to those around  $w$  since the former are in this case closer to the cations. Such an arrangement allows each Mg ion to have around it an almost complete double shell of water molecules, and the linking-up of these double shells produces layers in which two out of every three water sites are occupied. In this arrangement of the water layers, there are holes corresponding to triads of vacant water sites, each triad being equidistant from three cations with their associated double hydration shells. These sites may tend to be vacant (at normal temperature and pressure) because a water molecule in such a site would be in the third hydration shells of *two* cations and hence less stable than those associated with a single cation.

The types of bonding operating within the interlamellar region can now be considered with the aid of measurements taken from the contour map (Fig. 1*a*). If each water molecule (e.g.  $\text{H}_2\text{O}(A)$ , Fig. 8) is attached to its related oxygen by means of a hydrogen bond ( $\text{H}_2\text{O}-\text{O}$ , 2.84 Å), the second hydrogen can be directed towards another water molecule ( $\text{H}_2\text{O}(B)$ ) in the same sheet, so that the  $\text{H}-\text{O}-\text{H}$  angle is  $104\frac{1}{2}^\circ$  in agreement with the spectroscopically measured value (Darling and

\* Support for the assumption is provided by evidence of the occurrence of  $\text{Mg}^{2+}\cdot 12\text{H}_2\text{O}$  groups in salt solutions (Sidgwick, 1950, p. 237), and by the high energy of hydration of Mg cations.

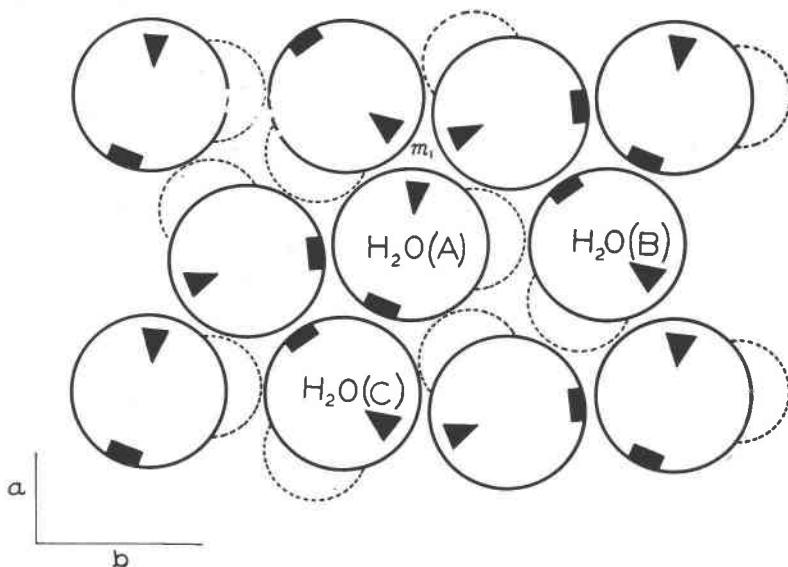


FIG. 8. Suggested system of weak hydrogen bonding illustrated for a single water sheet assuming all water molecule sites filled. Oxygens of water molecules represented by full circles, packing radius (Rees, 1949) to scale; hydrogens linked to silicate surface oxygens not shown; hydrogens in the plane of the water sheet represented by broken semi-circles; negative poles represented by black triangles and rectangles, triangles indicate greater displacement of charge from the plane of the sheet than rectangles.

Dennison, 1940). The second hydrogen lies in the plane of the water sheet but the two negative poles of the water molecule are slightly displaced therefrom, one directed towards the Mg ion site and the other pointing in the general direction of a third water molecule site ( $H_2O(C)$ ).

Since the intermolecular distances within a water sheet are either  $3.06 \text{ \AA}$  or  $3.40 \text{ \AA}$ , it is clear that normal hydrogen bonding does not operate at these points, and that the interactions are of a less specific nature. They may be regarded as *weak* hydrogen bonds and, as a consequence, a rigid application of tetrahedral linkages need not apply. In the vicinity of a cation site, the observed intermolecular distance within a water sheet of  $3.06 \text{ \AA}$  is greater than the value calculated for a perfectly regular octahedron of waters around a Mg ion (viz.  $2.92 \text{ \AA}$ ). The triads of water molecules associated with a cation are expanded slightly in the plane of the sheets so as to allow each water to approach its associated oxygen. As a consequence, the cations sink slightly into the water triads in both sheets and the intersheet distance of the water molecules is reduced to  $2.88 \text{ \AA}$  so as to preserve the Mg— $H_2O$  distance of  $2.06 \text{ \AA}$ . The intersheet distance of  $2.88 \text{ \AA}$  is uniform throughout the water

layers, which provides a possible further reason for the occurrence of triads of vacant water sites associated with the unoccupied  $v$  and  $w$  cation sites where the binding effect of the cations is absent. The observed intermolecular distance in an expanded triad of waters, viz. 3.40 Å, is consistent with the model if packing radii are assumed (Rees, 1949).

The idealised arrangement proposed above (Fig. 7) gives two out of three water sites occupied, which is approximately the required ratio, and the ratio of exchangeable cations to waters in the network is one in twelve which is close to the value indicated by the chemical formula (1:13.5). This model may therefore be closely approximated in the Mg-vermiculite under examination. A highly-ordered arrangement of the interlamellar region is not inconsistent with the observed ease of cation replacement (Milne and Walker, 1950), since normal diffusion processes can be expected to operate through vacant  $u$  sites and "interstitial" positions  $v$  and  $w$ , with concomitant adjustments in the water network. It is evident that the interlamellar region must be regarded as a dynamic system in which constant rearrangement and adjustment is taking place.

#### DISCUSSION

Detailed analysis has revealed a distortion in the surface oxygen network of the silicate layer in vermiculite. The explanation advanced is based on residual electrostatic forces acting between the central octahedrally-coordinated atoms and the surface oxygens of the silicate layers. Evidence for the existence of a distortion of the silicate layer in muscovite has been noted previously by Hendricks and Jefferson (1939), although in this case the data did not allow the nature of the distortion to be defined. Slight departures from regularity are therefore possible in silicate layers of this type.

The solution advanced for the stacking of the silicate layers, if valid, would impose certain limitations on similar minerals, and may therefore be applicable to the stacking sequences in talc and pyrophyllite. No satisfactory explanation for the  $0kl$ ,  $k \pm 3n$  spectra has so far been deduced for these minerals. The observed structure amplitudes of the  $02l$  reflexions in vermiculite have been shown to correspond closely to the values calculated not for  $q$  or  $r$  (Fig. 4) separately, but for the positional mean of these two possible arrangements. It is necessary to point out, however, that the results of the interpretation here placed on the diffuse reflexions cannot be reconciled with the theoretical treatment of disorder for cobalt in the region  $\alpha \sim \frac{1}{2}$  (Wilson, 1949, p. 70), which is analogous to the present case and predicts the almost complete disappearance of the diffuse regions. The discrepancy may arise from the failure of the theoretical

treatment to take into account the apparent increase in symmetry of the structure in the region  $\alpha \sim \frac{1}{2}$ .

The main interest attached to the structure analysis lies in the light which it throws on the organization of the interlamellar region. The water-cation network consists of two sheets of distorted hexagonally-linked water molecule sites with the cations occupying definite positions in the midway plane. Although the chemical data require that only one-third of cation sites ( $m_1$  or  $m_2$ ), and two-thirds of water sites should be occupied, it has been shown that a random filling of the available sites is not a necessary consequence of the data and, in the vermiculite under examination, a highly-ordered arrangement of the water molecules and cations is probable. In vermiculites which carry a higher population of exchangeable cations (Barshad, 1950, 1952), the idealised structure would be realised to a lesser extent, since  $u$ ,  $v$  and  $w$  sites would be expected to be partly occupied by cations and the distribution of the water molecules in the available sites would be altered accordingly. Nevertheless, grouping of the water molecules around the cations and a tendency towards a uniform distribution of the cations are to be expected in all similar minerals if the assumptions made above are valid.

It has usually been assumed, in considering the interaction of exchangeable cations with the planar surfaces of layer silicates, that the former are located by reactive spots of negative charge on the silicate layer surfaces arising from individual isomorphous substitutions. The present structure analysis has located the interlamellar  $Mg^{2+}$  ions in a plane midway between silicate layers. In this plane, the potential energy due to electrostatic forces can be shown by calculation to be effectively uniform, if the high frequency of isomorphous substitution is taken into account.\* The distribution of the cations in the midway plane is therefore not related to any *directive* effect of the electrostatic forces. The importance of the hydration behaviour of the cations in this respect is attested by the relationship between the cations and the water molecules as revealed by the diffraction data, and also by the observed spontaneous rehydration of partially-dehydrated Mg-vermiculite (Walker, 1949). In the interlamellar region, the water molecules within a sheet are linked by weak hydrogen bonds and the individual water sheets are held together by the cations. The hydrogen bonds binding the water molecules to the oxygen atoms of the silicate surfaces are probably stabilised to some extent by the electrostatic forces acting through the water molecules. We may conclude that, in Mg-vermiculite, the location of the

\* In vermiculite, which is a trioctahedral mineral, the substitution of about one in three tetrahedral and about one in five octahedral atoms gives rise to negative and positive charges respectively. The result is a net negative charge acting at the silicate layer surfaces.

water molecule sites is determined by the surface configuration of the silicate layers, and that the mutual relationship of the water sheets in a single water-cation layer is determined by the requirement for octahedral coordination of the water molecules around the cations. The unimportance of direct electrostatic interaction between the cations and surface oxygens is consistent with the conclusion of Guggenheim and McGlashan (1951) that the influence of next-nearest neighbours is entirely negligible. Their result, however, does not invalidate the proposed tendency to the formation of second hydration shells around the interlamellar cations in Mg-vermiculite, since each water molecule is equivalent in position with respect to the adjacent silicate layer surface and dipole interaction between water molecules can therefore exert a significant influence.

The structure derived for the interlamellar region in Mg-vermiculite, even in its less specific form, excludes the hypothetical water-layer structure proposed by Hendricks and Jefferson (1938*b*) for vermiculite, and later modifications made to take account of the exchangeable cations (e.g. Hendricks, Nelson and Alexander, 1940). Furthermore, the structure observed does not appear to have been considered in any of the models proposed for the water-cation network of layer silicate minerals.

#### ACKNOWLEDGMENT

The authors gratefully acknowledge helpful criticism by Dr. A. L. G. Rees, particularly with regard to the nature of the forces operating within the crystal lattice.

#### REFERENCES

- BARSHAD, I. (1948), *Am. Mineral.*, **33**, 655.  
 BARSHAD, I. (1949), *Am. Mineral.*, **34**, 675.  
 BARSHAD, I. (1950), *Am. Mineral.*, **35**, 225.  
 BARSHAD, I. (1952), *Proc. Soil. Sci. Soc. Am.*, **16**, 176.  
 BERNAL, J. D., AND FOWLER, R. H. (1933), *J. Chem. Phys.*, **1**, 515.  
 BRINDLEY, G. W. (1951), Chap. VI in X-RAY IDENTIFICATION AND STRUCTURES OF CLAY MINERALS, edit. G. W. Brindley, *Min. Soc., London*.  
 BRINDLEY, G. W., OUGHTON, B. M., AND ROBINSON, K. (1950), *Acta Cryst.*, **3**, 408.  
 BYSTRÖM, A., AND A. M. (1951), *Acta Cryst.*, **4**, 469.  
 DARLING, B. T., AND DENNISON, D. M. (1940), *Phys. Rev.*, **57**, 128.  
 GRUNER, J. W. (1934), *Am. Mineral.*, **19**, 557.  
 GRUNER, J. W. (1939), *Am. Mineral.*, **24**, 428.  
 GUGGENHEIM, E. A., AND MCGLASHAN, M. L. (1951), *Trans. Far. Soc.*, **47**, 929.  
 HENDRICKS, S. B., AND JEFFERSON, M. F. (1938*a*), *Am. Mineral.*, **23**, 851.  
 HENDRICKS, S. B., AND JEFFERSON, M. F. (1938*b*), *Am. Mineral.*, **23**, 863.  
 HENDRICKS, S. B., AND JEFFERSON, M. F. (1939), *Am. Mineral.*, **24**, 729.  
 HENDRICKS, S. B., NELSON, R. A., AND ALEXANDER, L. T. (1940), *J. Am. Chem. Soc.*, **62**, 1457.

INTERNATIONALE TABELLEN ZUR BESTIMMUNG VON KRISTALLSTRUKTUREN (1935), Berlin: Borntraeger.

KAAN, G., AND COLE, W. F. (1949), *Acta Cryst.*, **2**, 38.

MATHIESON, A. McL. (1951), *J. Scient. Instr.*, **28**, 112.

MATHIESON, A. McL., AND WALKER, G. F. (1952), *Clay Mins. Bull.*, **1**, (8), 272.

MILNE, A. A., AND WALKER, G. F. (1950), *Trans. Fourth Int. Cong. Soil Sci.*, **2**, 62.

MILNE, A. A., AND WALKER, G. F. (1951), *Clay Mins. Bull.*, **1** (6), 171.

REES, A. L. G. (1948), *J. Chem. Phys.*, **16**, 995.

SIDGWICK, N. V. (1950), *THE CHEMICAL ELEMENTS AND THEIR COMPOUNDS: Oxford.*

WADSLEY, A. D. (1952), *Nature*, **170**, 973.

WALKER, G. F. (1947), *Clay Mins. Bull.*, **1** (1), 5.

WALKER, G. F. (1949), *Nature*, **163**, 726.

WALKER, G. F. (1950a), *Mineral. Mag.*, **29**, 72.

WALKER, G. F. (1950b), *Nature*, **166**, 695.

WALKER, G. F. (1951), Chap. VII in *X-RAY IDENTIFICATION AND STRUCTURES OF CLAY MINERALS*, edit. G. W. Brindley, *Min. Soc., London.*

WEST, C. D. (1935), *Z. Krist.*, **91**, 480.

WELLS, A. F. (1950), *STRUCTURAL INORGANIC CHEMISTRY*, 2nd ed., *Oxford.*

WILSON, A. J. C. (1942), *Nature*, **150**, 152.

WILSON, A. J. C. (1949). *X-RAY OPTICS*, *London.*

*Manuscript received Feb. 18, 1953.*